V6 – Analyzing 3D chromatin conformation

Chromatin conformation has large implications on gene expression, but is usually ignored in expression analysis.

Program for today:

- 3D chromatin conformation
- Hi-C method
- Biases in Hi-C data analysis
- integrated analysis of multiple data sources

chromatin

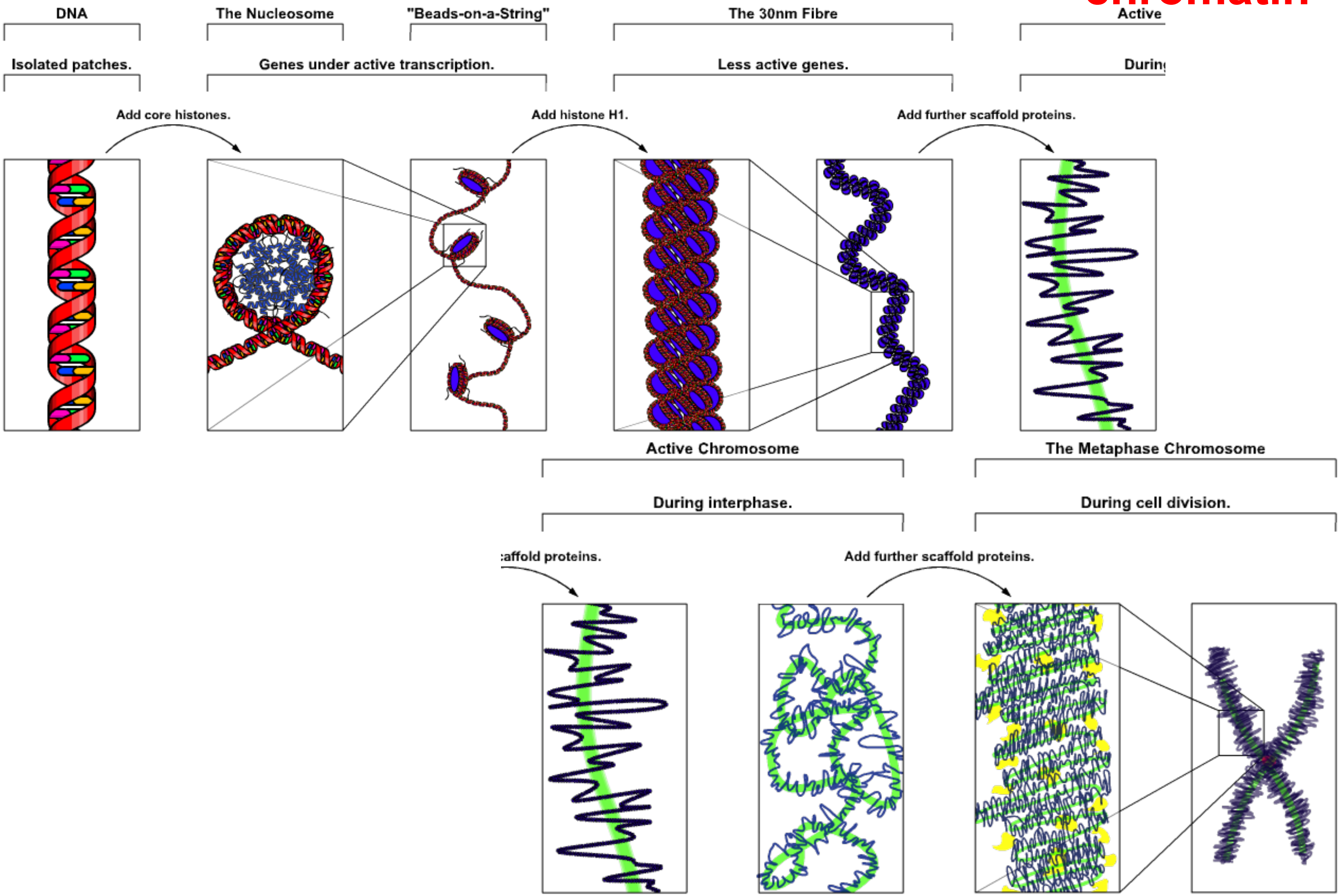

DNA
The Nucleosome
"Beads-on-a-String"
The 30nm Fibre
Active
Isolated patches.
Genes under active transcription.
Less active genes.
Durin
Add core histones.
Add histone H1.
Add further scaffold proteins.
Active Chromosome
The Metaphase Chromosome
During interphase.
During cell division.
affold proteins.
Add further scaffold proteins.

Chromosome Conformation Capture Technologies

DNA-protein cross-links

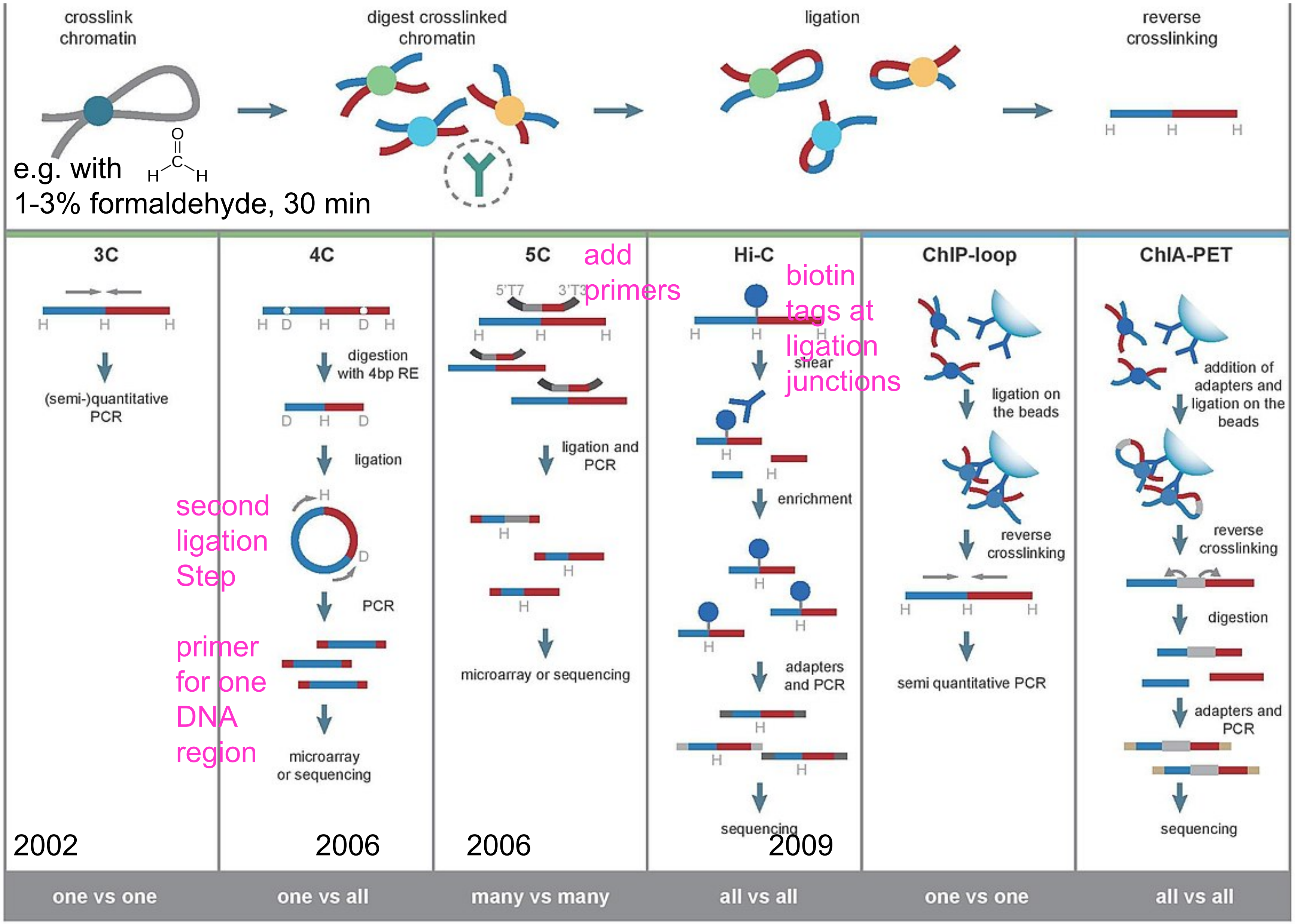

add primers

biotin tags at ligation junctions

second ligation Step

primer for one DNA region

2002 2006 2006 2009

www.wikipedia.org

3D Chromatin conformation: highest level

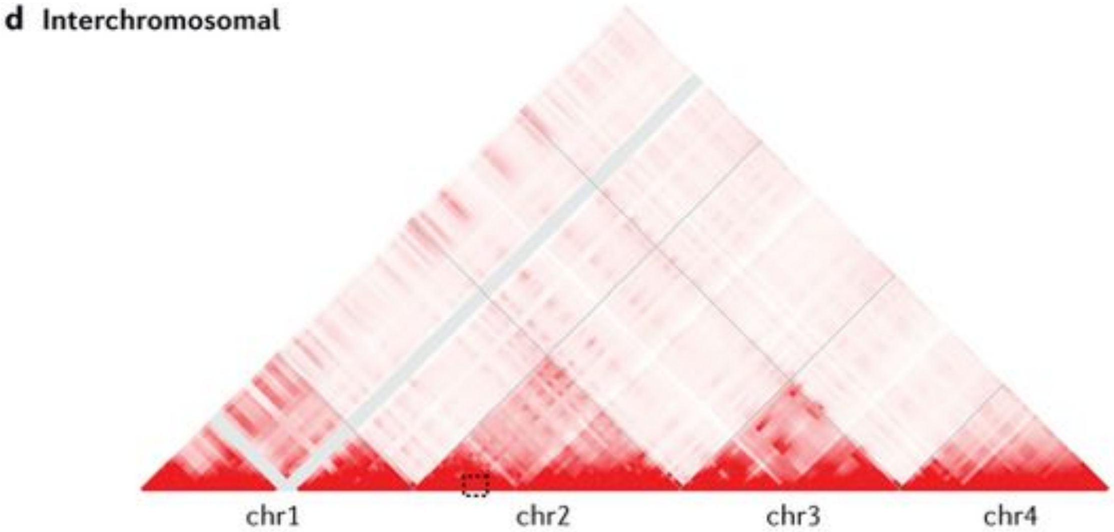

249 Mb 242 Mb 198 Mb 186 Mb

Data from human GM12878 cells (lymphoblastoid cell line). **Nucleus**

At the highest-level of 3D organization *trans*-interactions are rare and individual chromosomes (chrs) occupy distinct **territories** (denoted by irregular shapes) within the nucleus (grey circle).

Gene-rich chromosomes are preferentially found inside the nuclear core and gene-poor chromosomes are localized close to the nuclear membrane.

Bonev & Cavalli, *Nature Rev Genet* **17**, 661–678 (2016) |

3D Chromatin conformation: 50 kb resolution

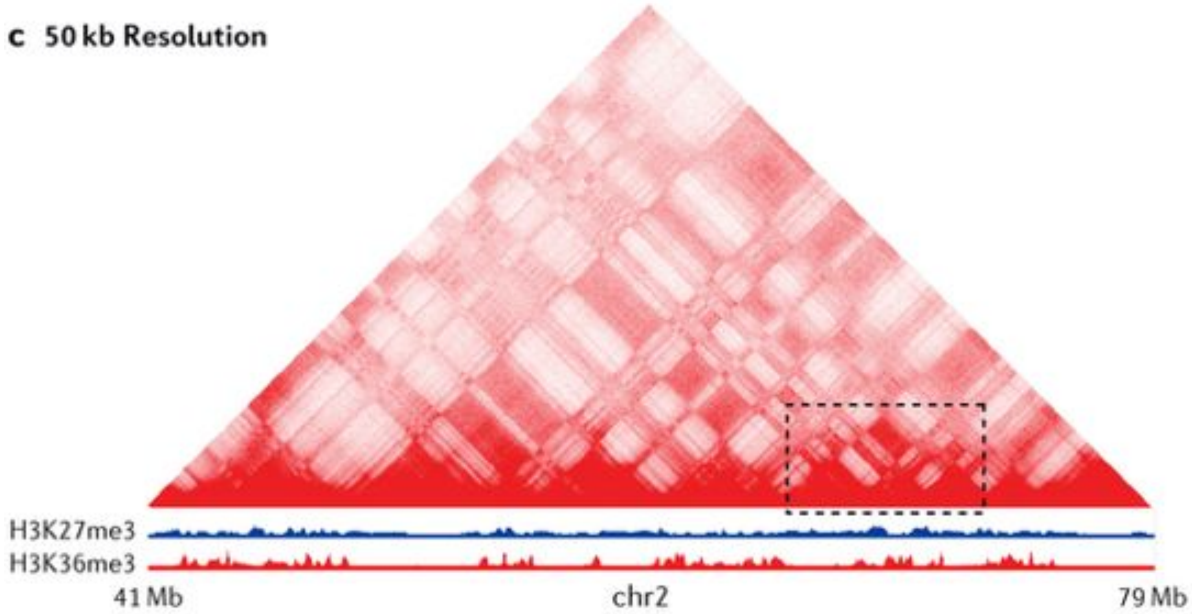

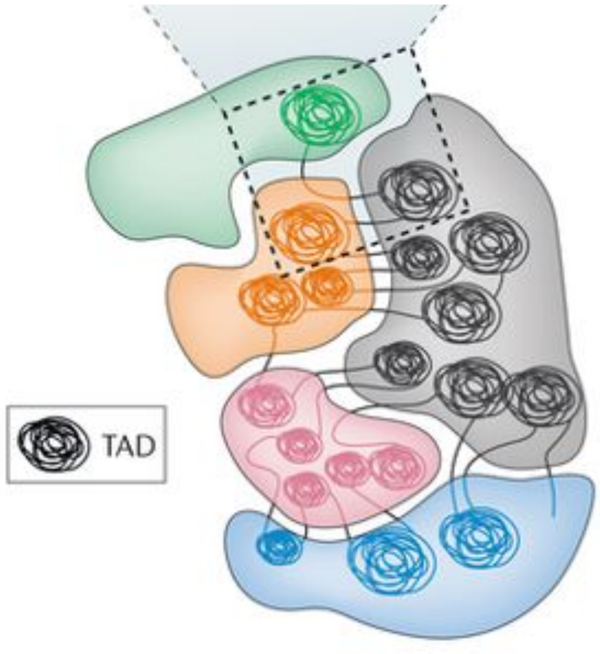

Different topological domains with similar epigenetic signatures are characterized by stronger inter-domain interactions.
They are organized into **compartments**.

Here, blue and grey represent the active compartment, whereas interactions between green, orange and red **topologically associating domains** (TADs) form the inactive compartment.

Bonev & Cavalli, *Nature Rev Genet* **17**, 661–678 (2016) |

3D Chromatin conformation: 10kb resolution

(left) ca. 8 Mb region containing several TADs that are manually annotated with solid lines.

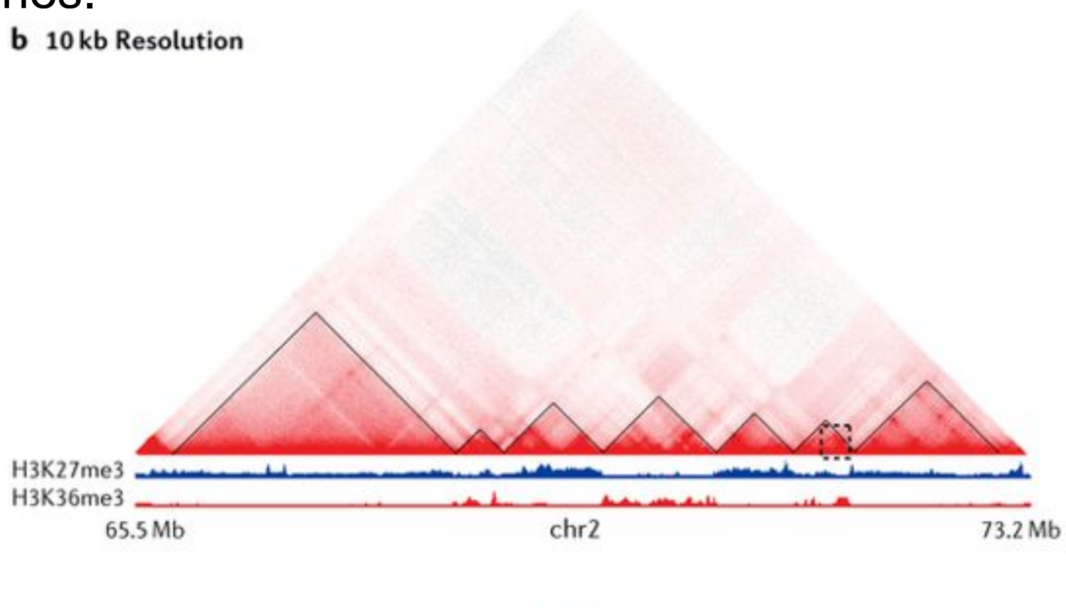

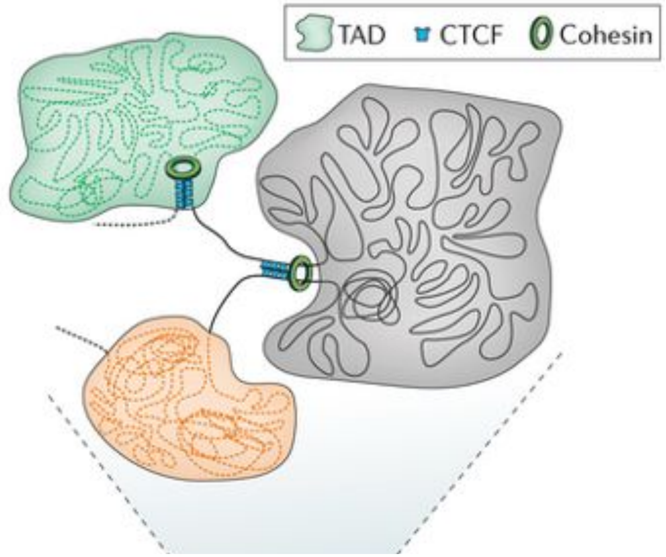

(right) 3 different TADs, enriched for either active marks (H3K4me3 and H3K36me3; grey), Polycomb (H3K27me3; green) or heterochromatin (H3K9me3; orange) are schematically represented in the 3D space.
CTCF proteins are shown as blue rectangles and loop-extrusion complexes (potentially cohesin) are depicted as green circles.

Bonev & Cavalli, *Nature Rev Genet* **17**, 661–678 (2016) |

3D Chromatin conformation: 5kb resolution

(right) Examples of different types of chromatin loops that can potentially reside within a domain

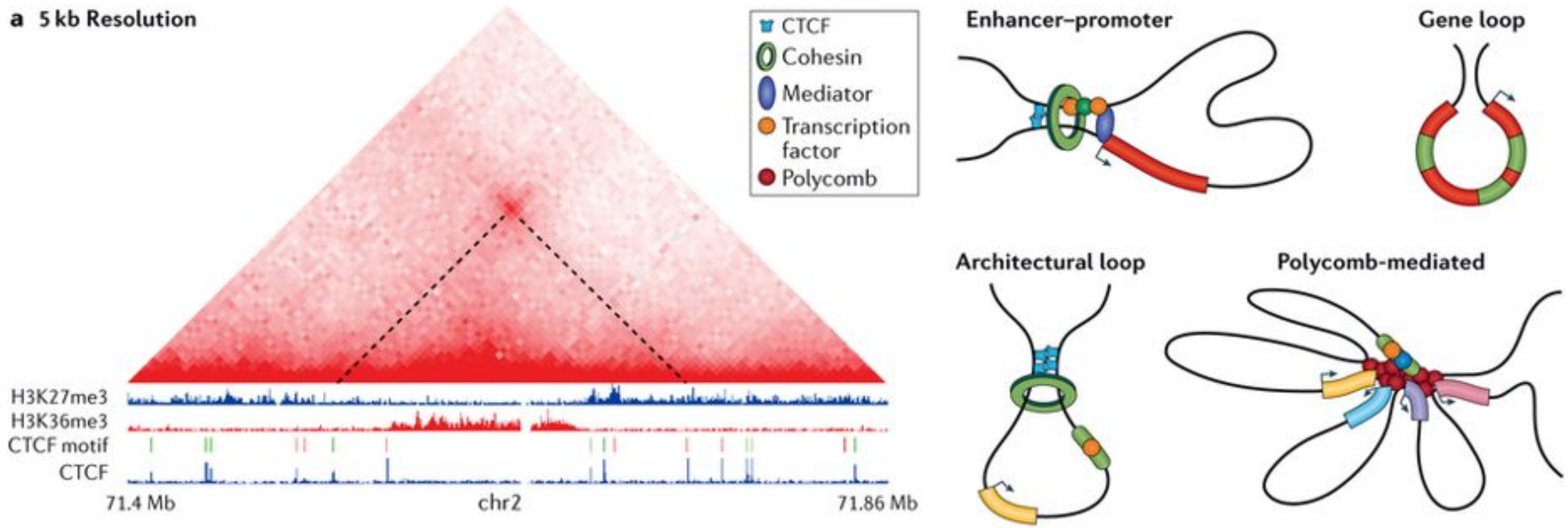

(left) : example of an architectural loop as seen in high-resolution Hi-C data (regions participating in loop formation are demarcated with dotted lines),
as well as CCCTC-binding factor (CTCF)-binding profile and CTCF motif orientation.

Bonev & Cavalli, *Nature Rev Genet* **17**, 661–678 (2016) |

Data from HiC

$n \times n$ contact matrix, where the genome is divided into n equally sized bins.

The value within each cell of the matrix indicates the **number of pair-ended reads** spanning between a pair of bins.

Depending on sequencing depths, the commonly used sizes of these bins can range from 1 kb to 1 Mb.

The bin size of Hi-C interaction matrix is also referred to as '**resolution**',

Owing to high sequencing cost, most available Hi-C datasets have relatively low resolution such as 25 or 40 kb, as the linear increase of resolution requires a quadratic increase in the total number of sequencing reads.

Zhang et al. *Nature Commun* **9**, 750 (2018)

Biases in computational analysis of Hi-C data

Procedures including crosslinking, chromatin fragmentation, biotin-labelling and re-ligation can all introduce **biases** that complicate the interpretation of observed contact frequencies.

Efficient and effective removal of multiple systematic biases is critical for the success of any subsequent analysis of C-data as well as for the proper interpretation of results.

Schmitt et al. Nature Rev Mol Cell Biol (2016) 17, 743

Random collisions affect chromosome capture data

Detection of an interaction between two loci does not necessarily mean that they are engaged in a functional looping interaction.

-> loci along a chromatin fiber will also randomly, and quite frequently, collide as the result of the inherent flexibility of chromatin.

In general, the frequency of **random collisions** is inversely related to the **genomic distance** between loci (larger "search space" for larger radius).

Thus, relatively frequent but nonfunctional interactions should always be observed for loci separated by small distances.

For sites separated by larger genomic distances, this 'background' signal decreases rapidly, but remains detectable for sites separated by as much as 150 kb.

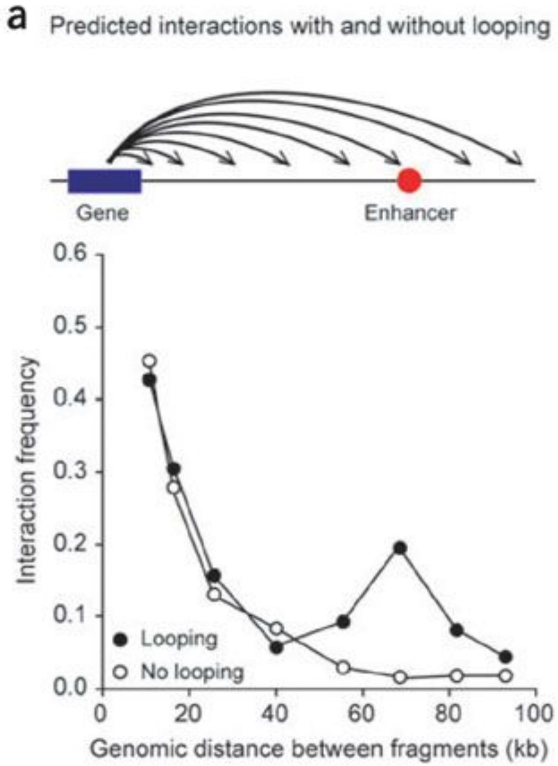

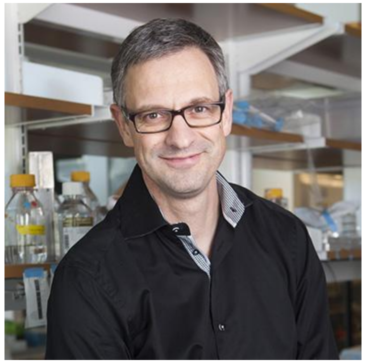

Job Dekker, *Nature Methods* **3**, 17–21 (2006)

Persistence length of DNA

The persistence length is a basic mechanical property quantifying the stiffness of a polymer.

The persistence length, P, is defined as the length over which correlations in the direction of the tangent are lost.

Let us define the angle θ between a vector that is tangent to the polymer at position 0 (zero) and a tangent vector at a distance L away from position 0, along the contour of the chain.

It can be shown that the expectation value of the cosine of the angle falls off exponentially with distance,

$$\langle \cos\theta \rangle = e^{-(L/P)}$$

where P is the persistence length and the angled brackets denote the average over all starting positions.

Bare double-helical DNA has a persistence length of about 39 nm.

For comparison, a nucleosome has dimensions of 6 × 10 nm.

www.wikipedia.org

Specific contacts affect neighboring loci

A specific contact between two elements located on two different chromosomes—in this example between centromeres—will also bring neighboring fragments into closer proximity, and thus they can nonspecifically interact.

Failure to determine a local peak in interaction frequencies may result in incorrectly concluding that two elements specifically interact,

whereas in reality it is their neighbors that are engaged in a specific interaction.

In this example, only the interaction between the two centromeres may be specific (-> highest peak) , whereas interactions with neighboring loci are likely the result of random collisions.

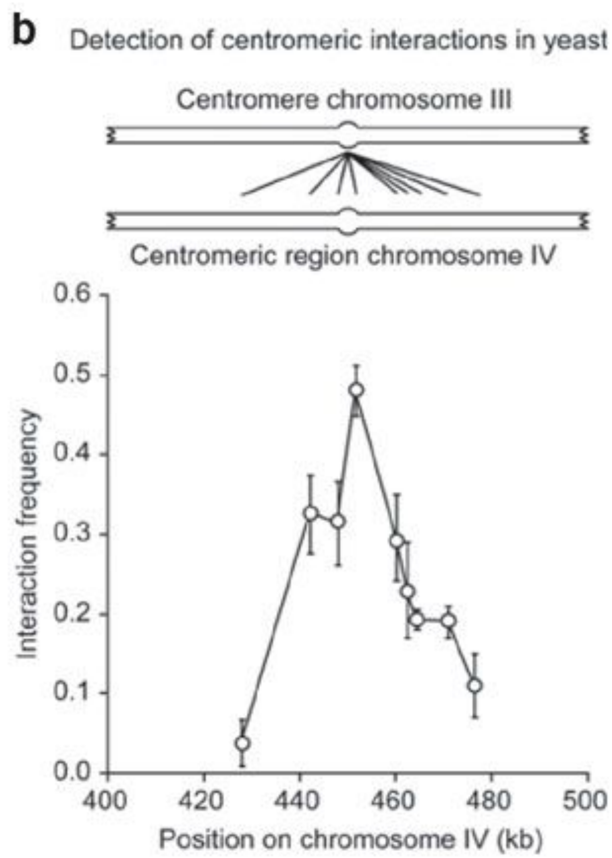

Job Dekker, *Nature Methods* **3**, 17–21 (2006)

Bias 1: restriction enzyme fragment length

HindIII 78%, NcoI 88% - 2 restriction enzymes

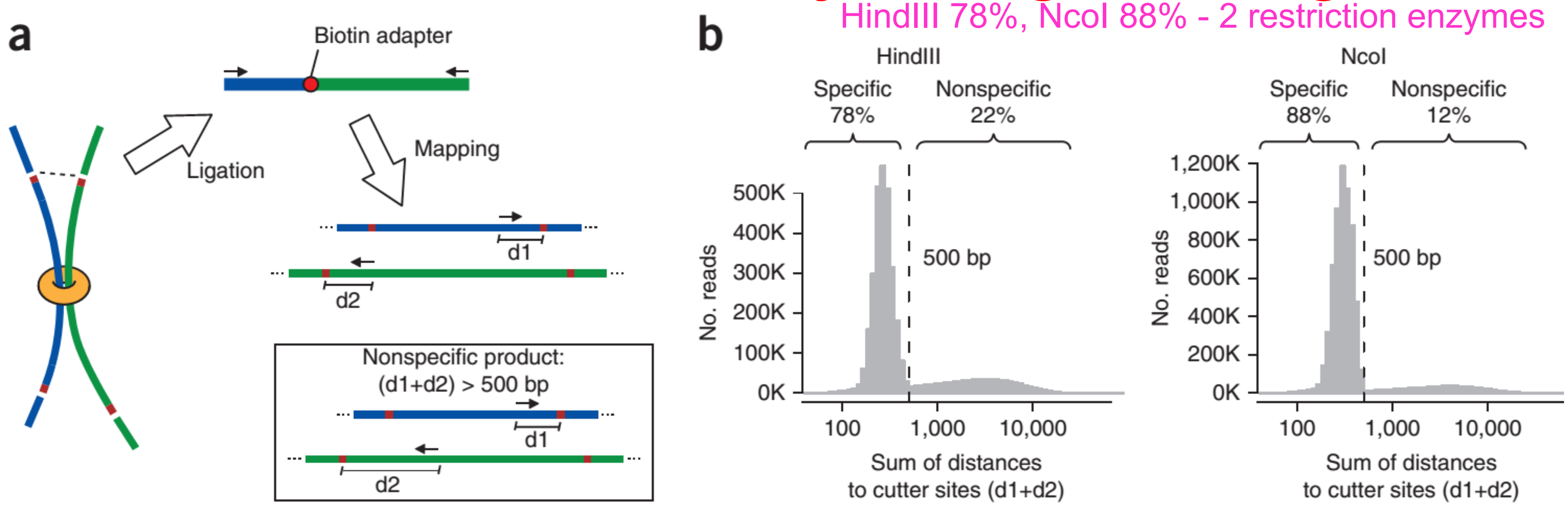

Hi-C ligation products (shown schematically in **a**) are expected to map near restriction sites because of size selection.

(**b**) For each Hi-C paired read, the sum of distances is computed from mapped Hi-C sequences to the nearest restriction sites. Shown is the distribution of distances.

Two distinct populations of reads are observed, one distributed as expected for normally ligated and size-selected products and one including reads mapped farther away from restriction sites.

Solution: discard reads with distance > 500 bp

Yaffe, Tanay Nature Genet (2011) 43, 1059

Bias 2 : GC content

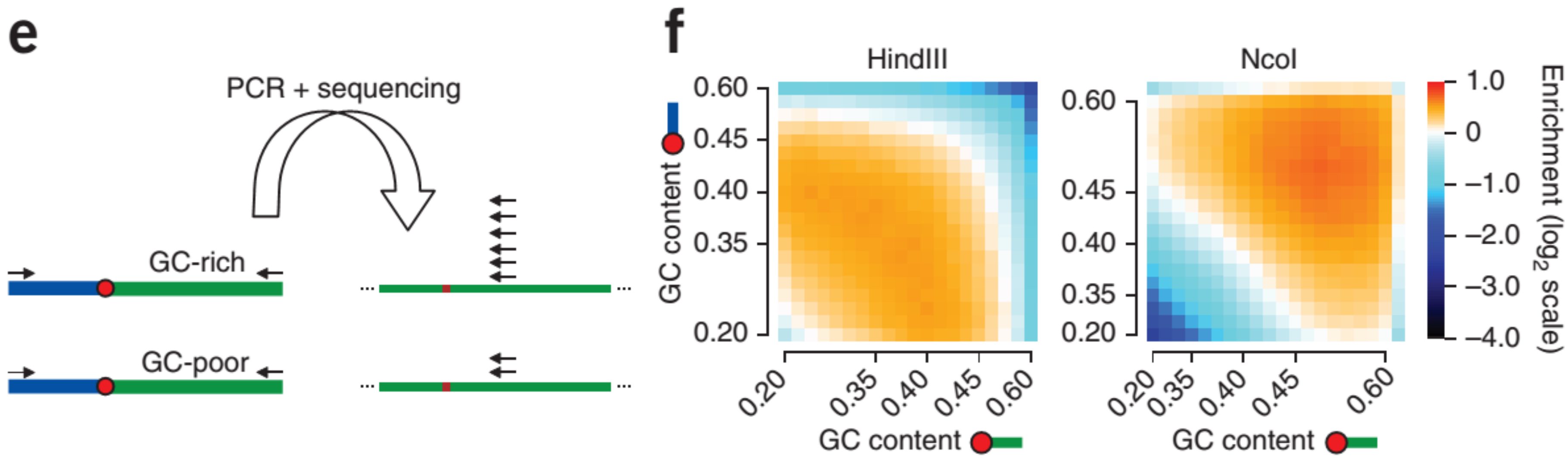

(**e**) Ligation product processing and sequencing may be biased by GC content.

In this example, the GC-rich region produces many more reads.

(**f**) Plotting the GC content of the 200 bp near the restriction fragment ends for *trans*-contacts shows intense and contrasting GC biases for the HindIII and NcoI experiments:

NcoI "prefers" GC-rich sequences, HindIII disfavors them.

Yaffe, Tanay Nature Genet (2011) 43, 1059

Bias 3 : sequence mappability

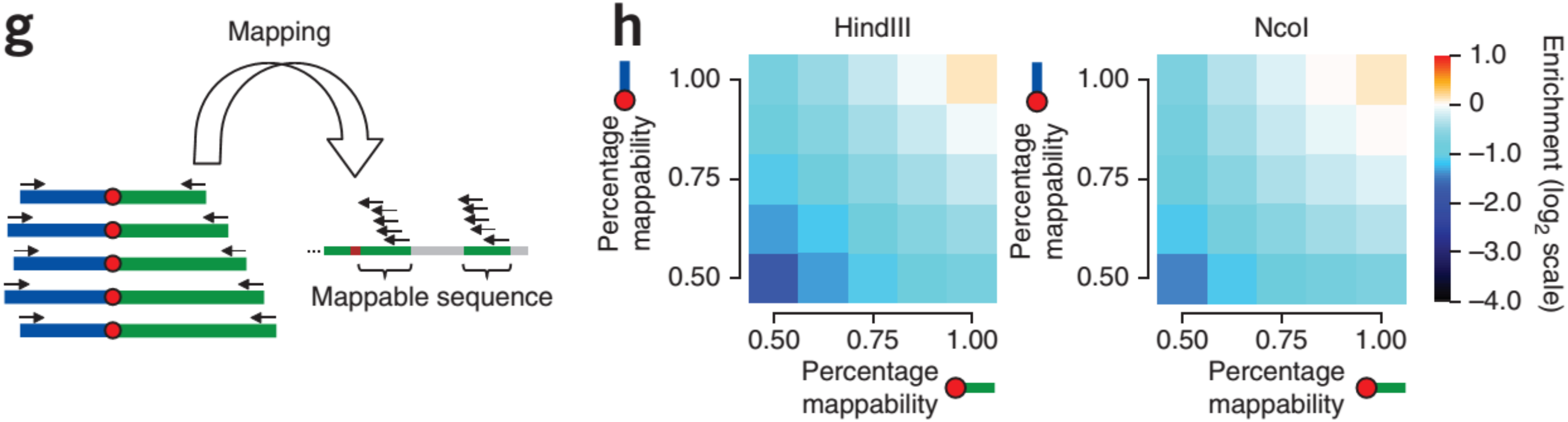

(**g**) Effect of sequence uniqueness. Different fractions of uniquely mappable short tags are observed next to restriction sites.

As shown in **h**, this has a direct empirical linear effect on Hi-C coverage.

Mappability is predicted and confirmed (**h**) to have a linear effect on the estimated *trans*-contact probabilities.

Yaffe & Tanay correct for biases 2 & 3

by a maximum likelihood approach.

Yaffe, Tanay Nature Genet (2011) 43, 1059

Biases in computational analysis of Hi-C data

In general, there exist two types of approaches to account for biases in C-data.

(1) account for biases in an explicit fashion — by assuming that all sources of systematic biases are known based on biases determined empirically from the observed data.

(2) account for biases in an implicit way — by assuming no known source (or sources) of bias, and assuming that the cumulative effect of the bias is captured in the sequencing coverage of each locus (or 'bin').

As Hi-C is a genome-wide assay, the implicit models assume that each locus should receive **equal sequence coverage** after biases are removed.

Implicit models all rely on some implementation of **matrix-balancing algorithms**.

Schmitt et al. Nature Rev Mol Cell Biol (2016) 17, 743

HiCnorm tool

HiCnorm corrects for these 3 biases using Poisson regression.

Poisson regression assumes that the response variable *Y* has a Poisson distribution, and assumes that the logarithm of its expected value can be modeled by a linear combination of unknown parameters.

If $\mathbf{x} \in \mathbb{R}^n$ is a vector of independent variables, then the model takes the form

$$\log(\mathrm{E}(Y \mid \mathbf{x})) = \alpha + \beta'\mathbf{x},$$

where $\alpha \in \mathbb{R}$ and $\beta \in \mathbb{R}^n$. Sometimes this is written more compactly as

$$\log(\mathrm{E}(Y \mid \mathbf{x})) = \boldsymbol{\theta}'\mathbf{x},$$

where $\mathbf{x}$ is now an $(n + 1)$-dimensional vector consisting of n independent variables concatenated to a vector of ones. Here $\boldsymbol{\theta}$ is simply α concatenated to $\boldsymbol{\beta}$.

Hu et al. Bioinformatics 28, 3131-3133 (2012)
www.wikipedia.org

Matrix balancing

A matrix is **unbalanced** if the L2 norm of some rows and their corresponding columns are different by orders of magnitude.

$$\|\boldsymbol{x}\|_2 := \sqrt{x_1^2 + \cdots + x_n^2}.$$

Some computations such as the computation of eigenvalues are numerically unstable if the matrix is unbalanced.

Given an unbalanced matrix A, the goal of **matrix balancing** is to find an invertible diagonal matrix D such that DAD^{-1} is balanced or approximately balanced in the sense that every row and its corresponding column have the same norm.

Schmitt et al. Nature Rev Mol Cell Biol (2016) 17, 743

Matrix balancing approaches

Implicit, matrix-balancing approaches have been widely used to account for biases in Hi-C data. They rely on two different assumptions.

(1) the combinatorial-bias effect between two interacting loci can be simplified as the product of the two locus-specific bias effects.

(2) if there is no bias effect (that is, when all bias has been accounted for), the total genome-wide contact summation for each locus will be a constant, implying that each locus has 'equal visibility' to the Hi-C assay.

Schmitt et al. Nature Rev Mol Cell Biol (2016) 17, 743

Matrix balancing approaches

Two matrix-balancing algorithms are:

Vanilla coverage: To account for bias, the observed contact frequency between locus A and locus B is divided by the product of the total genome-wide contact frequency at locus A and the total genome-wide contact frequency at locus B.

This ratio is used as the normalized contact frequency.

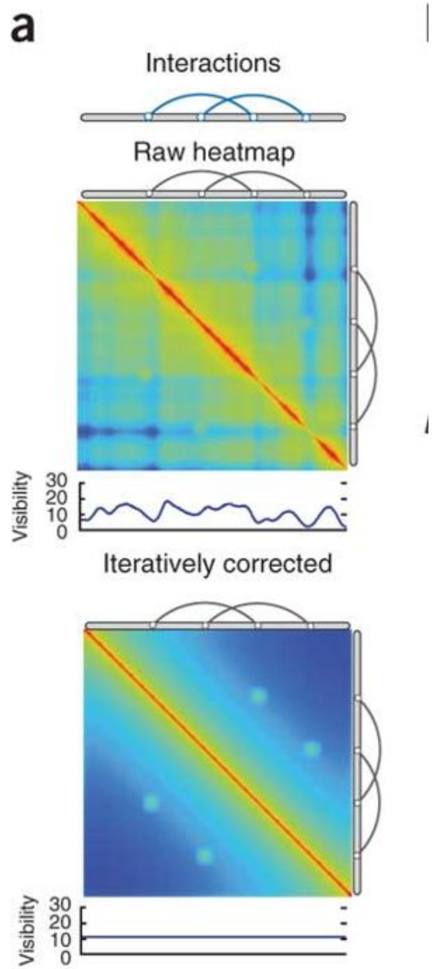

Iterative correction and eigenvector decomposition (ICE):

this process iterates through the vanilla coverage procedure (using updated total genome-wide contact frequencies!) until there is convergence of the normalized contact frequency.

+ reduced coverage variability from locus to locus

- greatly increased computational cost.

Schmitt et al. Nature Rev Mol Cell Biol (2016) 17, 743
Imakaev et al. Nature Methods 9, 999–1003 (2012)

Application of 4 bias removal methods: full chromosome

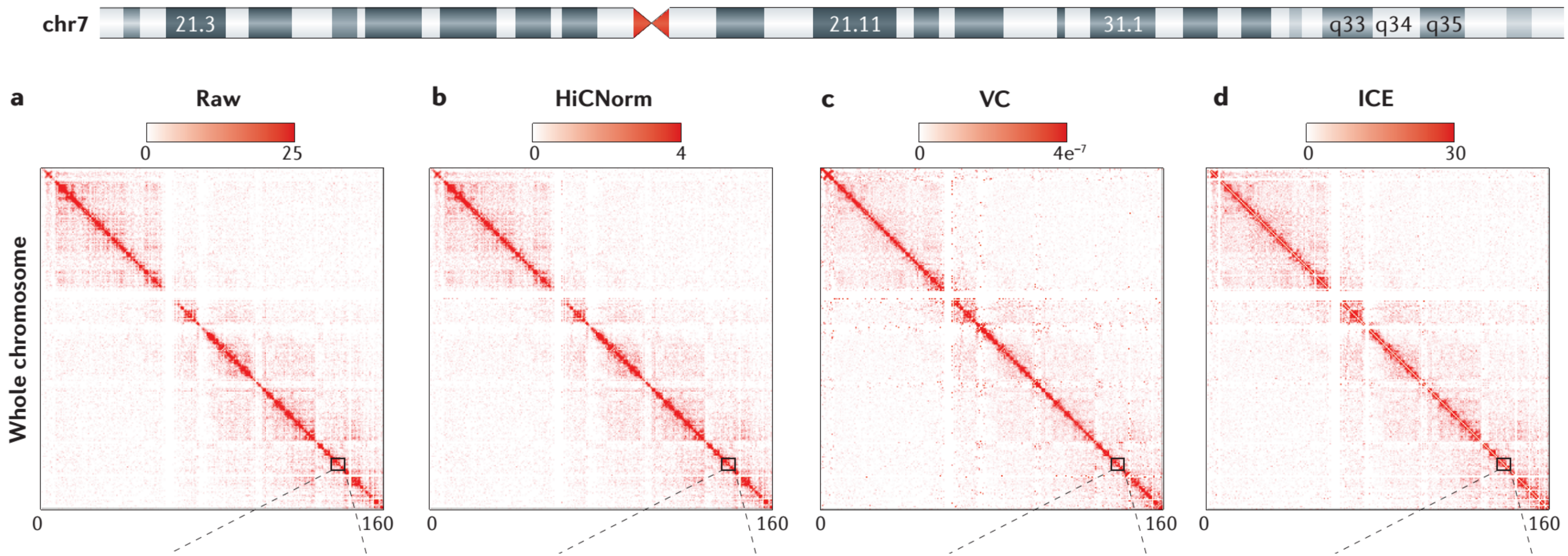

High-resolution Hi-C data from IMR90 cells were processed uniformly until the bias-removal step, at which point either raw contact matrices were generated or normalization was conducted with one of three methods.

Shown is data for whole human chromosome 7 for a raw Hi-C contact matrix (part **a**), an explicit model of bias removal (HiCNorm) (part **b**), and two methods of matrix-balancing algorithms for bias removal, vanilla coverage (VC) (part **c**) and iterative correction and eigenvector decomposition (ICE) (part **d**).

Schmitt et al. Nature Rev Mol Cell Biol (2016) 17, 743

Application of 4 bias removal methods: TAD domains

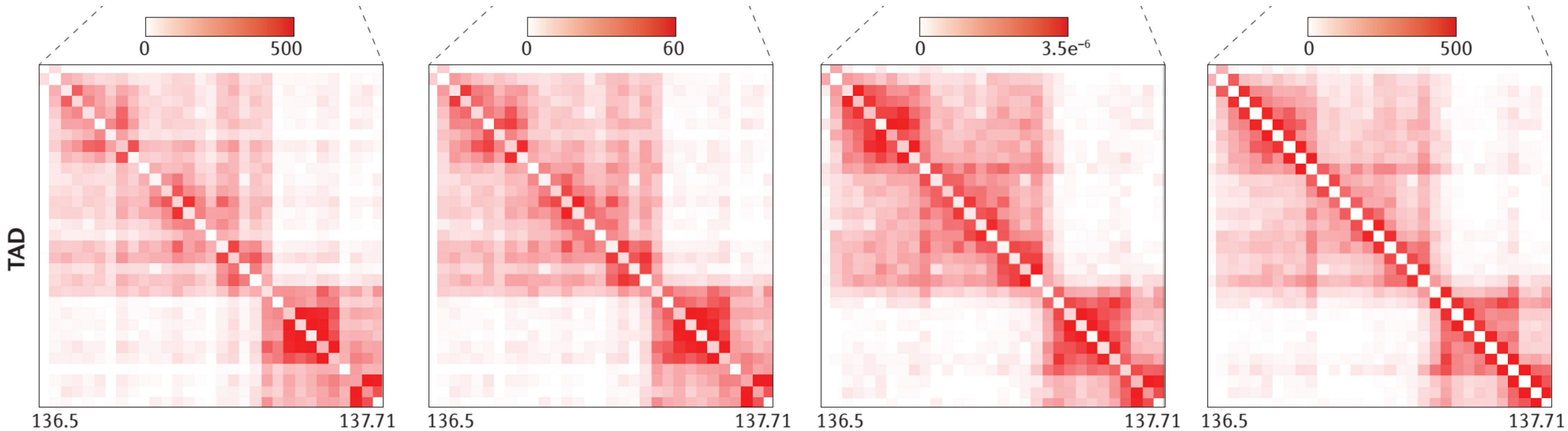

Pairwise interactions observed at higher frequency are depicted as a darker red colour along the colour gradient, whereas light red coloration represents very few observed interactions in the Hi-C data.

Different normalization methods yield slightly differences but very different numbers.

It is currently unclear which method works best.

Schmitt et al. Nature Rev Mol Cell Biol (2016) 17, 743

Integration of multiple data sets

The group of Frank Alber/USC has originally constructed a 3D model of the nuclear pore complex via data integration.

They now work on 3D models of chromatin.

lamina-DamID experiments identify specific chromatin domains with a high propensity to be located at the nuclear envelope (NE).

Chromosome conformation capture experiments (Hi-C and variants) detect chromatin interactions at a genome-wide scale.

Li et al. Genome Biology (2017) 18:145

lamina-DamID experiments

Schematic illustration of DNA adenine methyltransferase identification (DamID) experimental pipeline.

(a) Dam only or Dam fused to a protein of interest (POI) (blue) is expressed in a suitable cell type or transgenic organism. **Here: POI is lamin B1 that is part of the nuclear lamina → DAM localizes to nuclear membrane**

(b) Genomic DNA is extracted. DNA obtained includes N6-adenine methylation sites (Me) catalyzed by Dam.

(c) Genomic DNA is digested by the methylation sensitive restriction enzyme, DpnI.

(d) Digested fragments are amplified by polymerase chain reaction (PCR).

(e) Representative output indicating chromatin binding of a protein of interest at an individual locus. Vertical bars indicate the $\log_2$ ratio of Dam-fusion/Dam only.

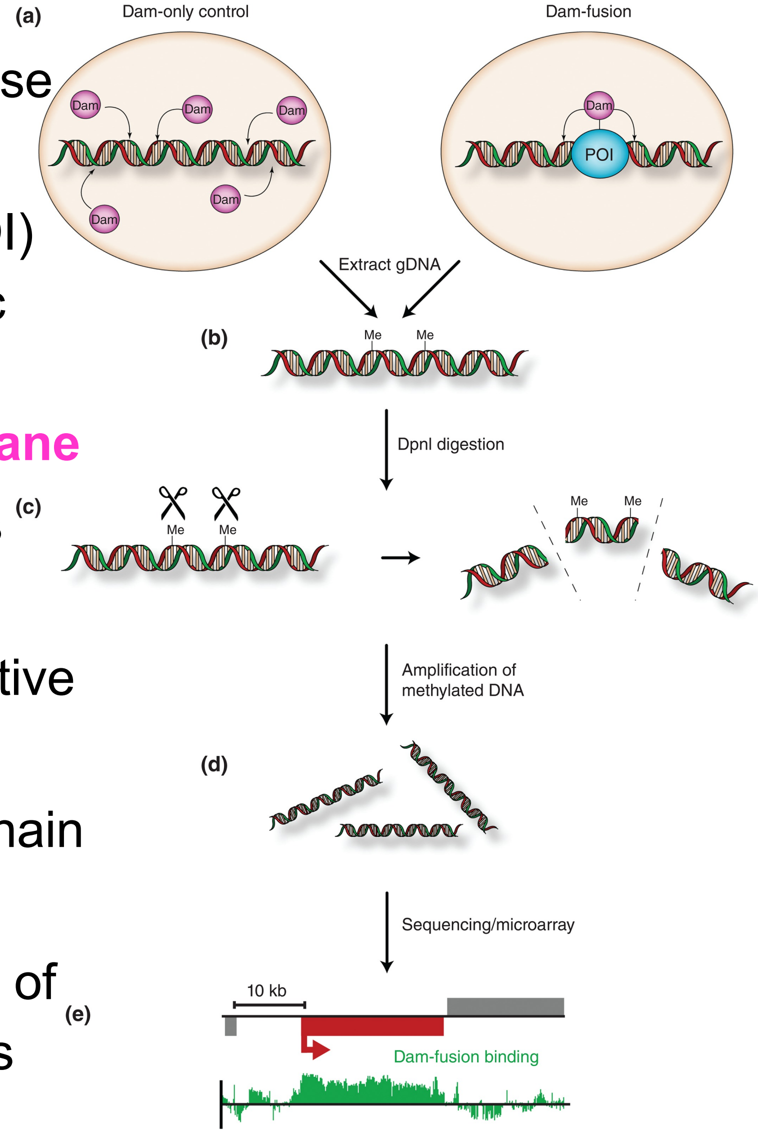

WIREs Dev Biol (2016) 5:25 – 37.

Integration of multiple data sets

So far, most population convolution models of genome structures have typically relied on just **one data type**, such as Hi-C, even though a single experimental method cannot capture all aspects of the spatial genome organization.

However, data are available from several technologies with complementary strengths and limitations.

Integrating all these different data types should increase the accuracy and coverage of genome structure models.

Moreover, such models would offer a way to cross-validate the consistency of data obtained from complementary technologies.

Li et al. Genome Biology (2017) 18:145

Integration of multiple data sets

For example, lamina-DamID experiments show a chromatin region's probability to be close to the lamina at the nuclear envelope,

whereas Hi-C experiments reveal the probability that two chromatin regions are in spatial proximity.

Large-scale 3D fluorescence in situ hybridization (FISH) experiments show the distance between loci directly, and can be used to measure the distribution of distances across a population of cells.

Li et al. Genome Biology (2017) 18:145

Drosophila melanogaster

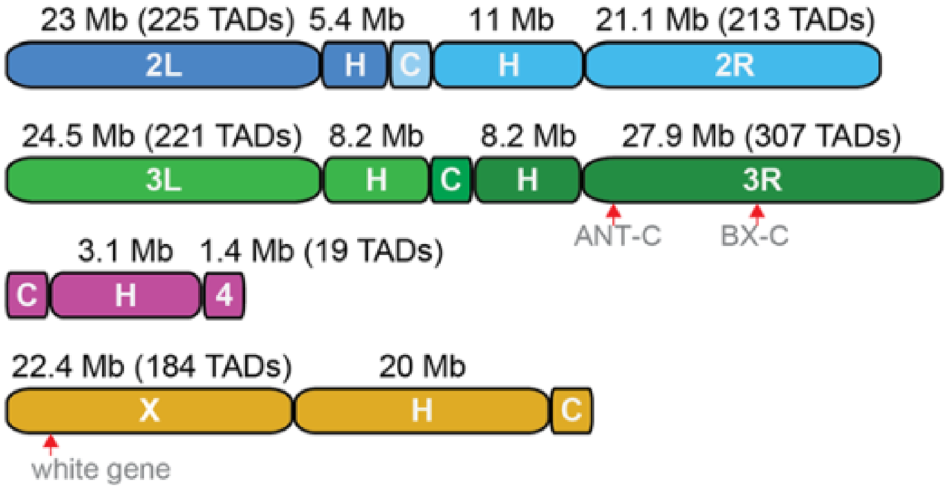

The genome of *D. melanogaster* (sequenced in 2000, and curated at the FlyBase database) contains 139.5 million base pairs on four pairs of chromosomes: an X/Y pair, and three autosomes labeled 2, 3, and 4.

It contains around 15,682 genes.

The euchromatin genome was divided into **1169 physical domains** based on Hi-C interaction profiles.

www.wikipedia.org

Integration of multiple data sets

Suppose **A** is a probability matrix derived from Hi-C data.
Its elements describe how frequently a given pair of TADs are in contact with each other in an ensemble of cells.

E is a probability vector derived from lamina-DamID data.
Its entries describe how frequently a given TAD is in contact with the nuclear envelope (NE).

The goal is to generate a population of genome structures **X**, whose TAD–TAD and TAD–NE contact frequencies are statistically consistent with both **A** and E.

We formulate the genome structure modeling problem as a maximization of the likelihood P(**A**, E|**X**).

Li et al. Genome Biology (2017) 18:145

Consider population of chromatin conformations

The **structure population** is defined as a set of M diploid genome structures $\mathbf{X} = \{\mathbf{X}_1, \mathbf{X}_2, \ldots, \mathbf{X}_M\}$, where the *m*-th structure $\mathbf{X}_m$ is a set of 3D vectors representing the center coordinates of 2 *N* domain spheres.

The contact probability matrix $\mathbf{A} = (a_{IJ})_{N \times N}$ for N TAD domains is derived from the Hi-C data. Each element a_{IJ} is the probability that a direct contact between domains I and J exists in a structure of the population.

The contact probability vector $E = \{e_I | I= 1, 2, \ldots, N\}$ is derived from the lamina-DamID data and defines the probability for each TAD to be localized at the NE.

Li et al. Genome Biology (2017) 18:145

Integration of multiple data sets

Thus, the optimization problem is expressed as:

$$\hat{\mathbf{X}} = \arg \max_{\mathbf{X},\mathbf{W},\mathbf{V}} \log P(\mathbf{A}, E, \mathbf{W}, \mathbf{V}|\mathbf{X})$$

$$\text{subject to} \begin{cases} \text{spatial constraint I}: \text{ nuclear volume constraints} \\ \text{spatial constraint II}: \text{ excluded volume constraints} \\ \text{spatial constraint III}: \text{ chromosome pairing upper bound} \\ \text{spatial constraint IV}: \text{ consecutive domain constraint} \end{cases}$$

The log likelihood can be expanded as

$$\begin{aligned} \log P(\mathbf{A}, E, \mathbf{W}, \mathbf{V}|\mathbf{X}) &= \log P(\mathbf{A}, E|\mathbf{W}, \mathbf{V}) P(\mathbf{W}, \mathbf{V}|\mathbf{X}) \\ &= \log P(\mathbf{A}|\mathbf{W}) P(E|\mathbf{V}) P(\mathbf{W}, \mathbf{V}|\mathbf{X}) \end{aligned}$$

The “contact indicator tensor” **W** = $(w_{ijm})_{2N \times 2N \times M}$ is a binary, third-order tensor. It contains the information missing from the Hi-C data **A**, namely which domain contacts belong to each of the M structures in the model population and also which homologous chromosome copies are involved.

V = $(v_{im})_{2N \times M}$ specifies which domain is located near the NE in each structure of the population and also distinguishes between the two homologous TAD copies

Li et al. Genome Biology (2017) 18:145

Integration of multiple data sets

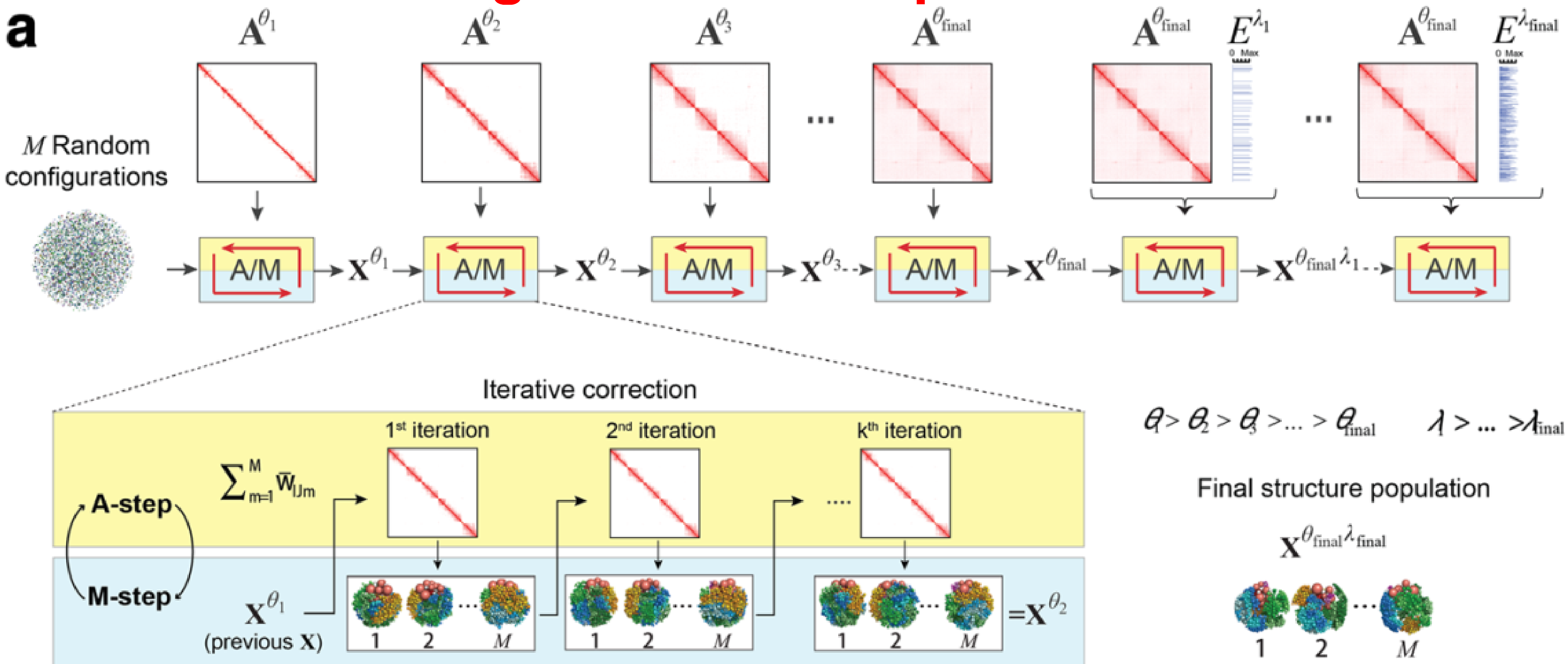

The initial structures are random configurations. Maximum likelihood optimization is achieved through an iterative process with two steps, assignment (A) and modeling (M). We increase the optimization hardness over several stages by including contacts from the Hi-C matrix **A** with lower probability thresholds (θ). After the population reproduces the complete Hi-C data, we include the vector E (lamina-DamID), again in stages with decreasing contact probability thresholds (λ).

Li et al. Genome Biology (2017) 18:145

Snapshot of a single structure picked from final population

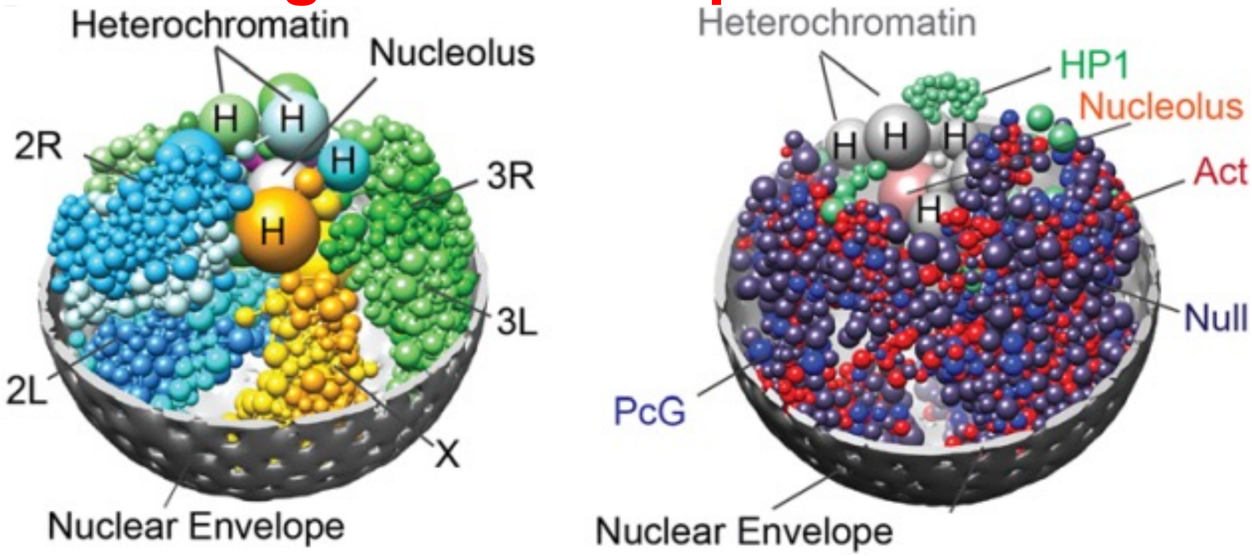

(left) The full diploid chromosomes are shown in colors: blue, chr2; green, chr3; magenta, chr4; orange, chrX.

The two homologs of the same chromosome are distinguished by the color tone, with one homolog copy with lighter and one with darker color. The heterochromatin spheres are larger than the euchromatin domains. The nucleolus is colored in silver.

(right) euchromatin domains are colored to reflect their epigenetic class:

red, active;

blue, PcG;

green, HP1;

dark purple, null.
Heterochromatin spheres are shown in grey and the nucleolus inpink

Li et al. Genome Biology (2017) 18:145

Independent control experiments (FISH)

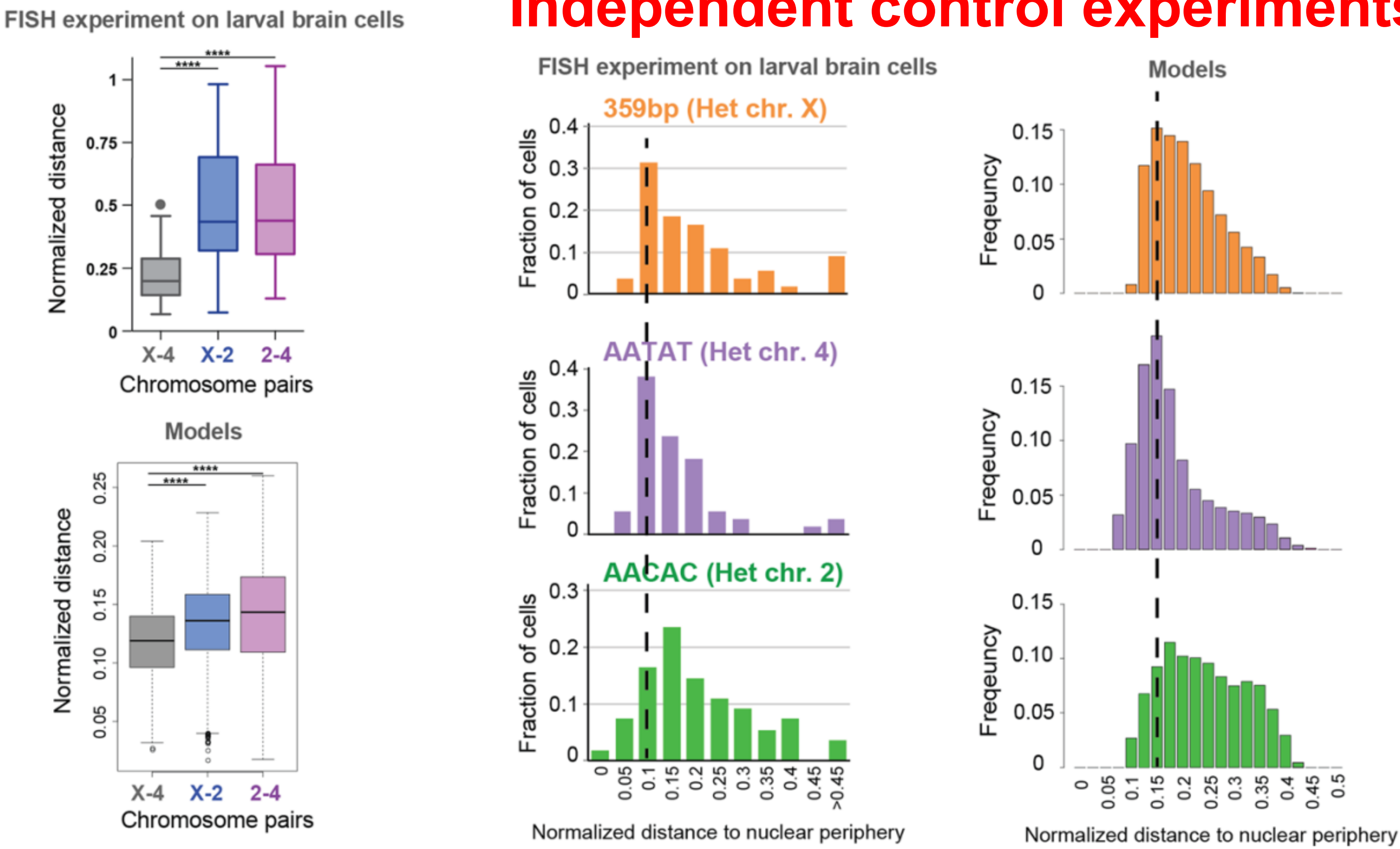

The model predicts certain location preferences for pericentromeric heterochromatin of individual chromosomes. We confirmed these predictions using FISH staining of heterochromatic repeated sequences (satellites) in *Drosophila* cells of larval brains.

Li et al. Genome Biology (2017) 18:145

Summary

Chromosome capture techniques enable to obtain information on **contacts** along one chromosome and between chromosomes.

Experimental design introduces various **biases** that must be corrected before analysis.

Data integration has great potential.

Considering **populations** of different structures helps to resolve conflicts between data.